Available online at www.sciencedirect.com
SCIENCE DIRECT
Journal of Photochemistry and Photobiology A: Chemistry 173 (2005) 169–173
Journal of Photochemistry and Photobiology A:Chemistry
www.elsevier.com/locate/jphotochem

# Optical response of thiosalicylic-capped CdS nanocrystals to terbium ions

C. Tiseanu [a,*], R.K. Mehra [b], R. Kho [b]

[a] National Institute for Laser, Plasma and Radiation Physics, P.O. Box MG-36, RO 76900, Bucharest-Magurele, Romania
[b] Environmental Toxicology Graduate Program, Department of Neuroscience, University of California, Riverside, CA 92521, USA

Received 26 July 2004; received in revised form 25 January 2005; accepted 31 January 2005
Available online 2 March 2005

**Abstract**

The effects of terbium ion addition on the optical spectra of CdS nanocrystals capped with thiosalicylic acid were investigated by means of absorption and steady-state photoluminescence spectroscopy. Upon terbium addition, the CdS absorption was modified around the first exciton peak while the CdS photoluminescence experienced selective enhancing and quenching processes. The results indicated that, most probably, the two types of changes are decoupled. The interpretation considered the key role played by the capping ligand in the optical response of nanocrystals to the lanthanide ions.


*Keywords:* CdS nanocrystals; Thiosalicylic acid; Terbium ions; Absorption; Photoluminescence

## 1. Introduction

Semiconductor nanocrystals (NCs) doped with lanthanide ions have attracted a lot of interest in recent years due to their various optical applications [1–8]. These materials combine the confinement properties of the nanostructure and interesting surface chemistry, with the electronic properties of the core-incorporated ions. In case of CdS or ZnS nanocrystals, substantial differences between the chemical and physical properties of lanthanides versus $Cd^{2+}$ or $Zn^{2+}$ ions prevent the successful incorporation of the luminescent lanthanides into the nanocrystals core [9,10]. As a consequence, the lanthanides are most probably distributed on the nanocrystals surface, bound to the capping ligand or dispersed in the outer matrix containing the nanocrystals.

From an applications point of view, the surface-bound lanthanides might negatively affect the desired properties of the doped semiconductor nanocrystals [9]. They can, however, provide useful information on the various interactions occurring at the nanocrystals surface [11–14]. It is well known that the photoluminescence (PL) of quantum dots is strongly sensitive to the surface properties [15]. Therefore, the interaction of lanthanide's with the nanocrystal surface is expected to modify the emission properties. There are several reports on the photoluminescence response of quantum dots to various metal ions, mostly silent spectroscopic species, which act either as activators or quenchers ([16] and references herein). In contrast, similar studies employing lanthanide ions are very few, despite their potential use as luminescent probes for surface interactions.

The effect of lanthanide's in a colloidal system of surface-capped CdS and ZnS nanocrystals was recently studied by us in terms of the changes induced by the nanocrystal type on the PL dynamics of the terbium ion [13,14]. The results indicated that the terbium photoluminescence dynamics was strongly influenced by the nanocrystal type, and were explained on the basis of the coordination modes of the thiosalicylic acid with the $Cd^{2+}$ and $Zn^{2+}$ ions on the nanocrystals surface. In this work, the reverse effects, namely the changes induced by terbium doping on the optical properties of the thisoaslicylic-capped CdS nanocrystals, were scrutinized. The experimental methods made use of absorption and steady-state emission spectroscopy. The approach used in the investigation consid-

* Corresponding author. Tel.: +40 1 780 42 90; fax: +40 1 423 17 91.
*E-mail address:* tiseanuc@yahoo.com (C. Tiseanu).

1010-6030/$ – see front matter © 2005 Elsevier B.V. All rights reserved.
doi:10.1016/j.jphotochem.2005.01.017

ered the optical properties of the lanthanide ion, the capping ligand, and the semiconductor NCs as separate components as well as through their interdependencies.

## 2. Experimental

### 2.1. Synthesis

The highest purity terbium chloride (99.99%) was purchased from Sigma-Aldrich. Working solutions of terbium-TSA complexes were prepared in deionised water (Millipore). The terbium concentration was adjusted to $2 \times 10^{-5}$ M and the TSA concentration was varied between $10^{-5}$ M and $10^{-4}$ M. Series of aqueous colloidal CdS solutions were prepared using previously published methods [17]. Starting with a 0.075 M solution of TSA in 1 M Tris, $CdSO_4$ solutions were titrated to reach a 2:1 molar ratio of TSA:$Cd^{2+}$ in a final volume of 2 mL at pH = 10.4. To these TSA:metal complexes, an appropriate volume of sulfide as 1 M $Na_2S$ was added with vortexing to achieve an $S^{2-}$/metal ratio of 1.0. After thorough mixing, the samples were sealed and incubated for 60 min at room temperature. Terbium ions were added to the solutions of TSA-stabilized CdS NCs with the following values for the TSA/terbium concentration ratios: sample 0: no terbium; sample 1: 240/1; sample 2: 120/1; sample 3: 60/1.

### 2.2. Characterization

UV–vis absorption spectra were recorded on a Perkin-Elmer double-beam spectrophotometer (Lambda 3) controlled by PECSS software. Steady-state, excitation and PL spectra were recorded on a Perkin-Elmer LS50B spectrofluorimeter run by FLDM software at room temperature. Emission spectra were recorded using bandpass filters at appropriate wavelengths to minimize scattering and secondary emissions. The aqueous solutions of terbium-doped CdS NCs were stable for more than 4 months under air storage in the dark at room temperature.

## 3. Results and discussion

Bifunctional ligands used to passivate nanocrystals have the benefit of two functional groups that may contribute to surface, chemical and optical properties. One functional group, for example, can bind to and protect the nanocrystals surface, and the other can be used to manipulate the surface for desired properties. Alternatively, both functional groups may contribute together to the overall surface properties. Among bifunctional ligands, thiosalicylic acid is a bidentate representing both ‘hard’ and ‘soft’ donors with carboxylic (–COOH) and thiol (–SH) groups in the 1, 2 positions (Scheme 1). [18].

In water, only the –COOH group of TSA is considered to bind the ion, since sulphur chelators are not expected to displace the strongly bound water molecules. In contrast, $Cd^{2+}$ ions at the nanocrystals surface are expected to bind both to the –SH and –COOH of the TSA [19].

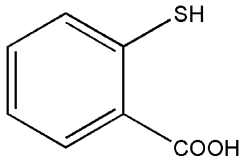


Scheme 1. Functional structure of the TSA molecule.

Fig. 1 presents the absorption and PL spectra of terbium-TSA complex under 290 nm excitation. The PL spectrum displays a broad, TSA-related PL emission centred on 400 nm, with the strongest 490 nm and 545 nm terbium PL transitions superimposed on the red tail of TSA emission. The sensitisation of the terbium PL in a region characterised by a negligible terbium absorbance, compared to that of the ligand (Fig. 1), indicates the coordination of terbium to the –COOH group of TSA [14].

### 3.1. Absorption

Illustrated in Fig. 2 are the absorption of undoped (sample 0) and terbium doped (samples 1–3) CdS nanocrystals. The absorption peak at ∼360 nm is typical for the CdS NCs with a ∼3 nm size and the onset is at 420 nm. With increasing terbium concentration, there is a clear tendency for dampening of the 360 nm centred peak (Fig. 2, left inset). A weaker spectral feature at about 336 nm can also be noticed in the valley of the absorption spectrum. Assuming a Gaussian inhomogeneous broadening mechanism, the deconvolution of the absorption spectra shows, in addition to peaks at 274 nm, 336 nm and 360 nm, a fourth peak centred at 389 nm (Fig. 2, right inset). Thus, what initially appeared to be a dampen-

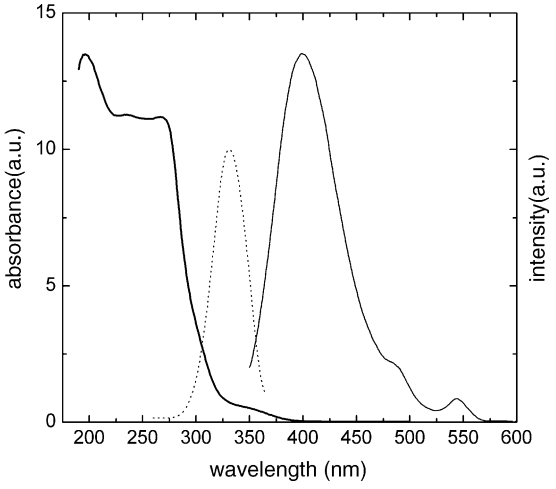


Fig. 1. Absorption, excitation and photoluminescence spectra of terbium-TSA complex. The PL excitation spectrum was measured at 545 nm (dotted line); photoluminescence spectrum of terbium-TSA complex was obtained at 290 nm lamp excitation.

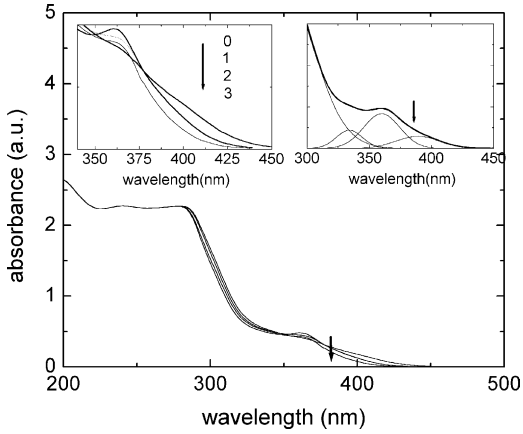


Fig. 2. Dependence of UV–vis absorption spectra of CdS nanocrystals on terbium concentration. Vertical arrow indicates the location of the excitation wavelength (380 nm). Left inset: dependence of the absorbance intensity in the 360 nm region on terbium concentration. Right inset: Gaussian deconvolution of the absorption spectrum of undoped CdS nanocrystals.

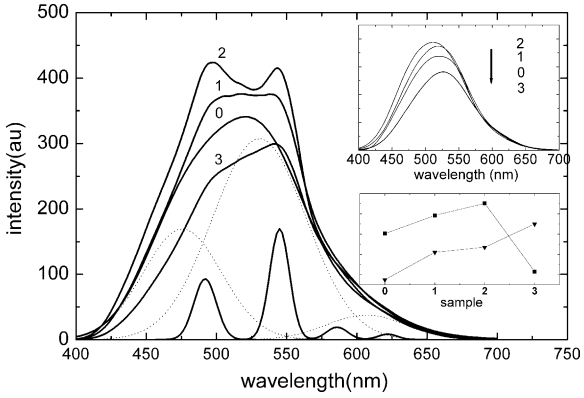


Fig. 3. Photoluminescence spectra of undoped (sample 0) and terbium-doped CdS nanocrystals (1–3) obtained under 380 nm excitation wavelength. The dotted lines represent the Gaussian deconvolution of the PL spectrum of the undoped CdS nanocrystals (sample 0), and of the terbium PL spectrum of sample 3 (see text). Top inset: dependence of the CdS PL on the terbium concentration. Bottom inset: dependence of the CdS integrated absorbance (►) and PL (■) measured between 350 and 450 nm and 400 and 700 nm, respectively on terbium concentration. Values were scaled to arbitrary units for comparison purposes.

ing of the 360 nm absorption peak was assigned to spectral redistribution within absorption from 350 to 450 nm.

Accordingly, the ratio of the 389 nm to 360 nm peak intensities increases with terbium concentration as follows: 0.42 in sample 0 (no terbium), 0.51 in sample 1, 0.62 in sample 2 and 1.10 in sample 3. The width of the 360 nm peak was slightly changed while the width of 389 nm peak increases from 34 nm in sample 0 to 55 nm in sample 3. As a result, the absorption onset was shifted to the red with almost 20 nm in sample 3 (Fig. 2).

The contribution of terbium absorption cannot account for the observed changes given the ∼1 to $10^5$ ratio of the absorption coefficients of terbium and CdS NCs in the 350–450 nm range [20,21]. We therefore interpret the observed changes in CdS absorption to be due to a process that involves the surface carboxyl group of TSA, which is interacting with and depends on the terbium concentration. The absorption properties are difficult to change through the modification of surface properties in a size range (∼3 nm) where confinement effects arise, Therefore, the increased terbium concentration could be causing a change in the size distribution of CdS nanocrystals, as evident by the presence of an absorption shoulder centred on 389 nm. Another source of altered absorption spectra could be the reduction, even in few percents, of the nanocrystal surface charge upon terbium binding to the TSA [22].

### 3.2. Photoluminescence

As shown in Fig. 3, the asymmetric PL profile of terbium-free sample begins at the absorption tail (∼390 nm) indicating band-edge emissions, and it extends up to the red region (ca. to 700 nm) with a maximum at 518 nm. Upon terbium addition, a superimposed structure related to the terbium PL transitions is observed in addition to the broad CdS emission. From the difference spectrum (not shown), two narrow width components (14–16 nm) were readily attributed to the 492 and 545 nm centred terbium transitions while a third, broader emission of ca. 60 nm width was assigned to the CdS emission.

Considering the above, as well as the shapes of the PL spectra of terbium-doped CdS nanocrystals (Fig. 3), we decided to extract the CdS-related PL spectra in presence of terbium ions. First, the shape of the undoped CdS PL was best fitted with three Gaussians centred on the blue (480 nm), green (530 nm) and red (600 nm) spectral regions, with the green contribution as the dominant emission (57%) (Fig. 3), while the blue and red emission accounted for 26% and 7% from the total PL intensity, respectively.

The blue and red emission accounted for 26% and 7% from the total PL intensity, respectively. Second, assuming that the PL spectra of terbium-doped nanocrystals were the algebraic convolution of the CdS-related PL and terbium-related PL, the CdS-related PL spectra in samples 1–3 were obtained using a two-steps Gaussian deconvolution: (1) the terbium-related PL was deconvoluted from the PL spectrum of terbium-TSA to obtain the peak values, widths and relative intensities, and (2) the peak values of the CdS-related PL were allowed to vary few nm around values obtained for sample 0. The agreement between the multi-Gaussian profile and the experimental PL curve was good in all samples. A small deviation of the fitted curve from the experimental data was attributed to the differences between terbium PL spectra induced by distinct coordination environments in CdS and TSA solutions [13,14]. This is reflected in the increased intensity of the hypersensitive transition $^5D_4$–$^7F_6$ relative to that of $^5D_4$–$^7F_5$ of terbium from 0.4 in TSA, to 0.48 in sample 1, 0.54 in sample 2 and 0.62 in sample 3. This trend shows that the environment of terbium ions in the CdS nanocrystal solution is more distorted than in the TSA solution, and that

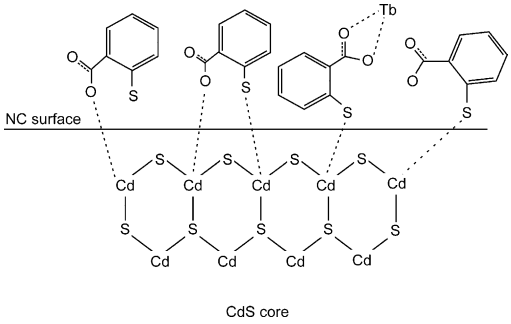


Scheme 2. Schematic representation of the TSA-capped CdS nanocrystals in presence of terbium ions.

the interaction between terbium and –COOH group on the nanocrystal surface intensifies with terbium concentration.

The deconvolution results also indicate that upon terbium addition, the blue emission of CdS centred on 480 nm is enhanced by 20% and 25% in samples 1 and 2, respectively, while it is quenched by almost 60% in sample 3 relative to the same emission in the undoped sample. The intensity of the green component centred on 530 nm was slightly modified in the range of ±5%, while the intensity of the red component centred on 600 nm remained basically unchanged with terbium addition. The latter emission was assigned a distinct temporal behaviour from the blue-green PL with measured lifetimes of up to 10 μs and with dependency on the emission wavelength [14]. Due to the increase and decrease of the blue component PL intensity, the CdS-related PL spectra were shifted to the blue (by 1 nm in sample 1 and 5 nm in sample 2) and to the red by 8 nm in sample 3 (Fig. 3, bottom inset), respectively.

There is little correlation between the terbium-induced changes of emission and absorption properties of the CdS nanocrystals. This is illustrated in Fig. 3, where the above changes are expressed in terms of dependency of the CdS emission maxima (top inset), the integrated CdS absorbance, and PL in the 350–450 nm and 400–700 nm regions (bottom inset) on the terbium concentration. It is well known that, besides size effects that dominate the absorption properties, the surface interactions dramatically influence the PL properties of nanocrystals [15,23,24]. Therefore, the interaction modes of the TSA with the CdS surface, as well as with terbium, ions are essential for understanding the emission behaviour. The proposed surface structure of TSA-capped CdS nanocrystals in the presence of terbium ions is illustrated in Scheme 2.

The TSA molecule binds on the CdS surface as a doubly $[SC_6H_4COO]^{2-}$ chelating ligand, binding to the neighboring surface cadmium atoms through both the thiol group and one of the oxygen atoms of the carboxylic acid group [19]. The maximum number of TSA capping ligands needed for the coverage of nanocrystal surface is thus decreased, and some TSA molecules exist momentarily as free ligands in solution. According to Dance [25], the carbonyl oxygen from the free TSA ligands and the primary thiol that binds cadmium forms a second coordination sphere. This second coordination sphere on the CdS surface is expected to increase its PL quantum efficiency due to better passivation. With increasing terbium concentration, competition between the lanthanide ion and the surface $Cd^{2+}$ ion for the carbonyl oxygen of free TSA molecules is likely to result in more of the electropositive terbium coordinating with the carbonyl. This may explain the quenching of the CdS PL in sample 3 (up to 20% in terms of overall PL decrease), with the majority of terbium ions bound to the TSA surface ligand [13]. The intricate nature of interactions between the TSA and CdS surface on the one hand, and TSA and terbium ions on the other, was already evidenced using time-resolved luminescence spectroscopy [13]. The PL lifetimes of terbium in CdS NCs solution were longer than those measured in TSA solution [13], and were explained by an increased protection of terbium ion against water molecules. It is possible that the decrease of CdS surface charge upon terbium addition also influences the nanocrystals PL. According to [26], the negative charge of the carboxyl groups of mercaptoacetate-capped CdS nanocrystals was found to play a positive role in the hole-trapping processes of the these nanocrystals. This was corroborated by a quick comparison with steady-state experiments on terbium-doped TSA-capped ZnS NCs obtained with an identical synthesis procedure [14]. The results indicated only a slight modification of ZnS PL in the presence of terbium ions.

A minimal decrease in the negative surface charge of ZnS nanocrystals is expected, given the relatively weak affinity of the –COOH group for $Zn^{2+}$ compared to $Cd^{2+}$ [27], which causes the ZnS surface to be more densely packed with carboxyl groups than in CdS NCs. As a result, in contrast with the CdS nanocrystals, the ZnS-related PL shows only a monotonic and uniform decrease with terbium concentration with a maximum quenching of ca. 5% in sample 3 (Fig. 4). Steady-state optical spectroscopy on the terbium-doped thiosalicylic capped ZnS nanocrystals is still in progress.

An alternative source for the quenching of CdS PL could arise from the energy transfer from the CdS surface to nearby

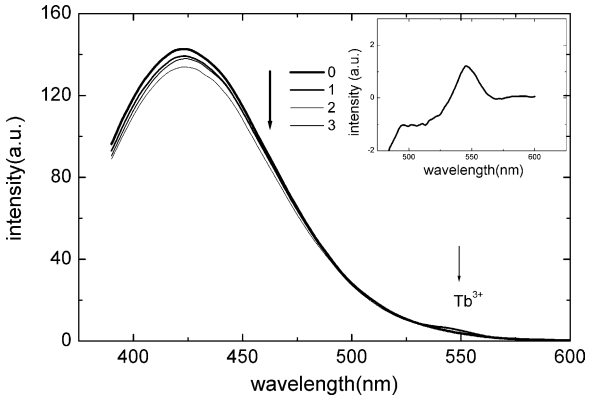


Fig. 4. Photoluminescence spectra of undoped (sample 0) and terbium-doped ZnS nanocrystals (samples 1–3) obtained under 310 nm excitation wavelength. Inset: difference PL spectra of terbium-doped (sample 3) and undoped ZnS nanocrystals.

terbium ions. Based on our previous analysis of terbium PL excitation spectra in TSA and CdS solutions [14] this possibility was neglected. Also, an apparent quenching due to the inner filter effect was ruled out due to the negligible absorption of terbium ions at 380 nm. The mechanism behind the activation effect, namely the terbium-induced enhancing of the CdS PL (up to 15% in term of overall PL increase) is not yet clear. A strong increase of the CdS PL when exposed to very dilute solutions of lanthanide β-diketonate complexes was explained by the interaction of the lanthanide complexes with cadmium vacancies on the nanocrystal surface [11]. However, the nanocrystals in that study were not capped, so a similar explanation in our system is not feasible. More, upon enhancement the emission maxima of CdS nanocrystals were shifted to the blue (top inset, Fig. 3), contrary to the expected size dependency of the nanocrystals PL. Since upon addition of the greatest amount of terbium (sample 3) caused the intensity of the CdS PL to decrease below the value of the undoped sample (Fig. 3), the activation process most likely co-exists with that of quenching in all samples. The observed terbium-induced changes of the CdS NCs photoluminescence are therefore described by a complex balance between activation and quenching processes, with the predominance of the activation process in samples 1 and 2, and of quenching process in sample 3. This behaviour is in sharp contrast with the effects induced by terbium addition on the TSA-capped ZnS nanocrystals, giving further evidence that the interaction mechanisms between the TSA and the CdS and ZnS nanocrystals are different.

## 4. Conclusions

Optical properties of thiosalicylic-capped CdS nanocrysrals were examined in the presence of three different terbium concentrations by means of steady-state optical spectroscopy. It was found that both the absorption and photoluminescence properties of the CdS nanocrystals depended on terbium concentration, and that the processes responsible for the changes are mostly decoupled. The changes in the absorption spectra were attributed to a process that involves the surface carboxyl group of TSA, which is interacting with and depends on terbium concentration. In emission properties, the terbium role as both enhancer and quencher of CdS photoluminescence was partially explained by considering the interaction modes between both –SH and –COOH groups of the thiosalicylic capping ligand with the CdS nanocrystals surface. Comparison to similar data for terbium-doped thiosalicylic capped ZnS nanocrystals further substantiated our interpretation. Experiments using a broader range of terbium concentrations, as well as combining steady-state and time-resolved spectroscopy, will enable a deeper understanding of the interaction mechanisms between chalcogenide nanocrystals and multifunctional ligands. Bifunctional ligands having roles in both passivation of nanocrystals and coordination to lanthanide ions will be explored further.

## References

[1] Y. Hori, X. Biquard, E. Monroy, L.S. Dang, M. Tanaka, O. Oda, B. Daudin Appl. Phys. Lett. 84 (2004) 206.
[2] M. Abdullah, T. Morimoto, K. Okuyama, Adv. Funct. Mater. 13 (2003) 800.
[3] A. Polman, F.C.J.M. van Veggel, J. Opt. Soc. Am. B 21 (2004) 871.
[4] A.J. Kenyon, Curr. Opt. Sol. St. Mater. Sci. 7 (2003) 143.
[5] Q.L. Liu, T. Tanaka, J.Q. Hu, F.F. Xu, T. Sekiguchi, Appl. Phys. Lett. 15 (2003) 4939.
[6] X.Y. Chen, H.Z. Zhuang, G.K. Liu, S. Li, R.S. Niedbala, J. Appl. Phys. 94 (2003) 5559.
[7] D. Pacifici, G. Franzo, F. Priolo, F. Iacona, L.D. Negro, Phys. Rev. B 67 (2003) 245301.
[8] S.M. Liu, F.Q. Liu, Z.G. Wang, Chem. Phys. Lett. 343 (2001) 489.
[9] A.A. Bol, A. Meijerink, Phys. Rev. B 58 (1998) 15997.
[10] N. Murase, R. Jagannathan, Y. Kanematsu, M. Watanabe, A. Kurita, K. Hirata, T. Yazawa, T. Kushida, J. Phys. Chem. B 103 (1999) 754.
[11] R.R. Chandler, J.L. Coffer, J. Phys. Chem. 95 (1991) 4.
[12] Y.F. Lee, M. Olshavsky, J. Chrysochoos, J. Less-Common Met. 148 (1989) 259.
[13] C. Tiseanu, R.J. Mehra, R. Kho, M. Kumke, Chem. Phys. Lett. 377 (2003) 131.
[14] C. Tiseanu, R.J. Mehra, R. Kho, M. Kumke, J. Phys. Chem. B 107 (2003) 12153.
[15] M. Gao, S. Kirstein, H. Mohwald, A.L. Rogach, A. Kornowski, A. Eychmuller, H. Weller, J. Phys. Chem. B 102 (1998) 8360.
[16] Y. Chen, Z. Rosenzweig, Anal. Chem. 74 (2002) 5132.
[17] C.L. Torres-Martínez, L. Nguyen, R. Kho, W. Bae, K. Bozhilov, V. Klimov, R.K. Mehra, Nanotechnology 10 (1999) 340.
[18] R. Murugavel, K. Baheti, G. Anantharaman, Inorg. Chem. 40 (2001) 6870.
[19] T. Lover, W. Henderson, G.A. Bowmaker, J.M. Seakins, R.P. Cooney, Chem. Mater. 9 (1997) 1878.
[20] W.T. Camall, in: K.A. Gschneider, L. Eyring (Eds.), Handbook on the Physics and Chemistry of Rare Earths, vol. 3, North-Holland, Amsterdam, 1979, p. 171.
[21] W.W. Yu, L. Qu, W. Guo, X. Peng, Chem. Mater. 15 (2003) 2854.
[22] E. Rabani, B. Hetenyi, B.J. Berne, L.E. Brus, J. Chem. Phys. 110 (1999) 5355.
[23] T. Ni, D.K. Nagesha, J. Robles, N.F. Materer, S. Mussig, N.A. Kotov, J. Am. Chem. Soc. 124 (2002) 3980.
[24] H. Zhang, Z. Zhou, B. Yang, M. Gao, J. Phys. Chem. B 107 (2003) 8.
[25] I.G. Dance, M.L. Scudder, R. Secomb, Inorg. Chem. 22 (1983) 1794.
[26] T. Uchihara, S. Maedomari, T. Komesu, K. Tanaka, J. Photochem. Photobiol. A 161 (2004) 227.
[27] F.M.M. Morel, Principles of Aquatic Chemistry, Wiley-Interscience, New York, 1983.